Optimal Control of Hybrid Power System Integrated with Distributed Generation and Electric Vehicle

Farhana Fayaz* and Gobind Lal Pahuja

NIT Kurukshetra, Haryana, India, 136119
E-mail: farhanafayaz23@gmail.com
*Corresponding Author

Abstract

This study presents load-frequency-control of a two-area hybrid power system (HPS) incorporating distributed generation, geo-thermal plant, thermal plant and electric-vehicle. Such a complex system with non-linearities leads the power system towards more complexity and accordingly requires a resilient controller to handle such complexity. In this regard, optimal cascaded proportional integral – multistage proportional integral derivative (cascaded PI-MSPID) is explored for developed power system. The efficiency of optimal controller is validated by comparing it with other controllers. The influence of flywheel energy storage on system dynamics is demonstrated. Further, the electric vehicle's participation in enhancing the system stability is presented. Moreover, the developed system is subjected to an intense load deviation which is a practical data taken from one of the literature. It is demonstrated that responses achieved for proposed cascaded PI-MSPID controller effectively handles the system disturbances, which reflects the strength of proposed cascaded PI-MSPID controller.

1 Introduction

The mismatch between the generation and load results in the deviation of system frequency and tie line power. For the reliable supply of power, the frequency and tie line power should be maintained at the nominal level. Load frequency control (LFC) aims at maintaining the frequency and tie line power at the scheduled level [1, 2]. LFC problem has been studied by many researchers and there exists ample amount of research in literature [3, 4].

The authors in [5] presented the dynamic frequency control for a two area thermal system. Frequency control of different multi-area thermal system using integral plus double derivative controller is presented in [6]. Automatic Generation Control of multi-area thermal system is reported in [7] where several parameters like integral controller gains, frequency bias parameters and governor speed regulation are optimized using bacterial foraging algorithm. The authors in [8] combined the robust control with an adaptive control technique and hence proposed a new resilient adaptive controller for the load frequency control of an isolated system. A novel method (based on Type-2 fuzzy system) for load frequency control of two-area interconnected thermal system was adapted by authors in [9] by considering generation rate constraint (GRC) and governor dead band (GDB). A cascaded Proportional Integral-Proportional derivative controller for the frequency control of four-area thermal system is proposed by authors in [10]. The Automatic Generation Control of interconnected hydrothermal system is presented in [11]. The authors in [12] proposed an optimal controller for the frequency control of interconnected hydro-thermal system. References [5–12] have discussed the frequency control of conventional power generation.

The majority of electric power comes from conventional generation like hydro and thermal power. The fossil fuels are depleting due to various factors such as overpopulation, overconsumption, deforestation, pollution etc. Alternate energy sources like wind and solar reduce the reliance on the fossil fuels and are considered as a green energy source since these reduce the environmental pollution. Hence, the renewable energy generations are being integrated to the existing power system [13–15]. The authors in [13] proposed a new secondary controller for the frequency control of three-area wind-thermal-hydro system. LFC of a hybrid power system (HPS) incorporating the photovoltaic system, wind turbine generator, diesel engine generator, battery energy storage system and superconducting magnetic energy storage is reported in [14]. In a HPS, the integration of distributed generation (DG) resources with the conventional generations meets the increased demand

of power. These DG's supply power to its nearby loads. Authors in [15] presented the LFC of the three-area thermal system by integrating DG resources in one of the areas. A robust controller for the load frequency control of HPS integrated with DG is reported in [16]. The authors have not considered the system nonlinearities. A genetic algorithm based controller for isolated hybrid generation/energy storage system consisting of solar thermal system, wind turbine generators, solar photovoltaic, fuel cells, diesel engine generators, battery energy storage system, flywheel, ultra-capacitors and aqua electrolyser is proposed in [17]. The authors in [18] incorporated geothermal power plant and also designed a controller for the conventional thermal, hydro, wind, and solar photovoltaic generations.

The power that is generated from renewable energy based systems like wind and solar is uncertain and intermittent in nature. In such systems, the frequency deviation due to the imbalance between the generation and demand is controlled by using energy storage systems (ESS). Hence ESS has an important role in maintaining the efficiency of electrical power when there is a mismatch between the supply and load demand due to the penetration of renewable energy sources. There exists literature on the frequency control supported by ESS. The type of energy storage devices that have been employed in the LFC of both conventional and deregulated systems include battery energy storage system [19], redox flow batteries [13], capacitive energy storage [20], superconducting magnetic energy storage [21] and flywheels [22] etc. Therefore, the authors are in view to incorporate the energy storage devices in the presented system.

The majority of the research present on the frequency control in renewable energy systems is employing battery as the storage device. However, the battery is expensive, requires maintenance and has a shorter life span. So, the researchers proposed a new storage technique (EVs) in order to control the frequency fluctuations in renewable energy systems. There exists little literature where EVs have been employed as a regulatory source in system dynamics control [23–25]. Hence there is scope for the implementation of EVs to highlight their regulating characteristic in hybrid power system.

Non-linearities in the power system makes it more practical, but they also create undesired oscillations. Further, the unpredictable nature of renewable resources and load demand variation further adds to the system's uncertainty. A robust controller is required to remove the disturbing influences caused by oscillations and uncertainty situations. Classical control [6], optimum control [26], adaptive control [27], robust control [28], and other systems have been proposed and developed to solve automatic generation control

(AGC) problem. As per the literature survey, basic proportional-integral (PI) controllers are commonly used in AGC due to their ease of implementation and ability to provide appropriate system response. Furthermore, advanced controllers including fractional-order [29], two-degree-of-freedom internal mode [30, 31], disturbance observer based [32], sliding mode [33, 34], cascaded [35–37] and model prediction [38] have been developed. In [39], the control of frequency for a hybrid power system is done using a multi-stage fuzzy logic proportional integral derivative controller. From the literature discussed above, cascaded and multi-stage based controllers in dynamic frequency control performed well over conventional controllers. Hence, the authors got motivation to apply cascaded multi-stage form of controllers.

Furthermore, as system parameters and loading circumstances change, the performance of fixed gain controllers reduces. Secondary controllers perform best when their gains and other parameters are optimized. Classical and meta-heuristic algorithms can both be used to find optimal values. Particle swarm optimization [40], firefly algorithm [41], ant colony optimization [42], marine predator algorithm [43], symbiotic organisms search algorithm [44, 45], back-tracking search algorithm [46], Jaya algorithm [47], grey wolf optimization technique [48], whale optimization algorithm [49], and other bio-inspired optimization techniques have been used in the LFC. A powerful bio-geography based krill herd (BBKH) optimization [50] is also available which is successfully used by the authors in [52] to optimize the different controller gains. Therefore, the present analysis is carried using BBKH as the optimization approach.

1.1 Objectives of the present Study

Based on the above discussion, the objectives of this study are mentioned below:

  I. Establishment of a matlab model for EV and DG based hybrid power system, in addition to the geo-thermal and conventional thermal plant. The cumulative model is modelled for load frequency control.
 II. Contemporaneous optimization of different secondary controllers viz. PID, multistage-PID, cascaded PI-PID and cascaded PI-multistage-PID (PI-MSPID) utilizing BBKH optimization technique.
III. To select optimal controller from secondary controllers mentioned in (II).
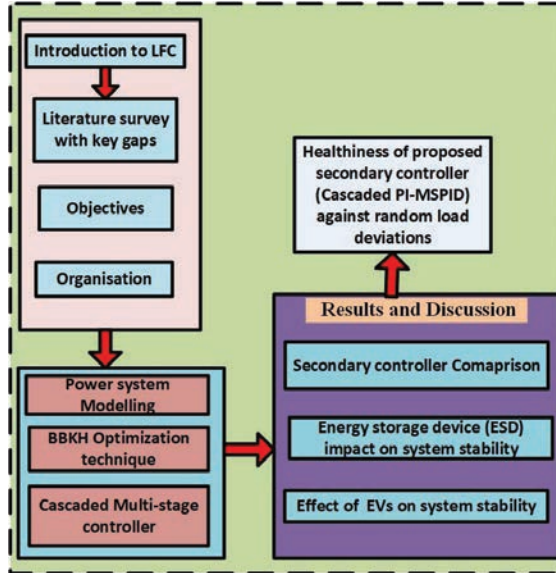IV. To inspect the system behaviour in existence of flywheel energy storage (FES).

Figure 1 Work flow presented in the manuscript.

   V. To examine the influence of EVs on system dynamic control.
  VI. To test the developed power system against practical load deviations.

1.2 Manuscript Organisation

The Figure 1 portrays the details of the work presented in this manuscript.

2 Power System Modelling

An unequal two-area HPS is chosen for examination. Area-1 incorporates DG in the form of wind-turbine-system and solar-thermal-system in addition to the thermal plant and EV while as area-2 incorporates thermal plant with additional generation support from the geo-thermal and EV. The Figure 2(a) portrays the linearized transfer function model of system considered while as Figure 2(b) portrays the transfer function model of DG. The capacity-ratio of two areas is taken as 1:2. An appropriate system non-linearities in the form of GRC (3% per minute) and GDB (0.06%)) is provided with thermal plants for realistic implementations. MATLAB Simulink software is used to develop the simulation model and execute the optimization codes. The system
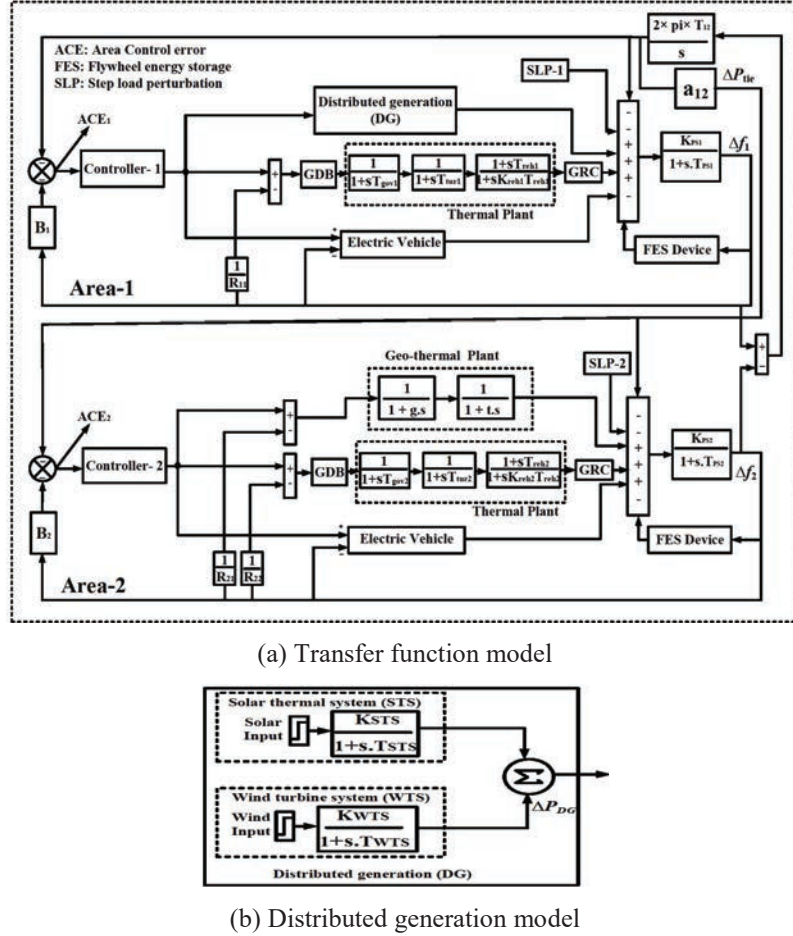
(a) Transfer function model

(b) Distributed generation model

Figure 2   Transfer function model of developed two-area power system with DG and EV.

nominal values are referred form [15, 18, 25]. The objective function for the study presented is integral squared error (ISE), given in (1).

$$ISE = \int_0^T [(\Delta f_i)^2 + (\Delta P_{tie-ij})^2]\, dt, i = 1, 2 \qquad (1)$$

The parameters in $= n$ (1) are;

(a) Output frequency deviation of each area "Δf_i" (i $=$ 1,2).
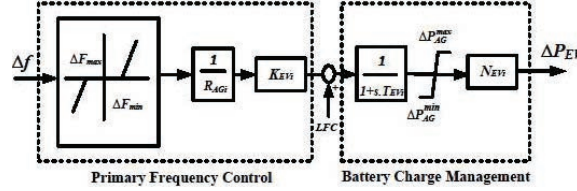(b) Tie-line power deviation between the two areas "$\Delta P_{tie-1-2}$".

Figure 3   EV simulation model [25].

2.1 Electric Vehicle (EV) Modelling

Figure 3 depicts the collective simulation model of EV incorporated in the presented work. It comprises of a battery charge management (BCM) which ensures of reliable power flow control among grid and battery. A circumstance can arise where EVs may get abruptly disengaged from the grid, leading to an unacceptable system performance. To handle such an issue, the frequency range is limited to ± 10 mHz. An EV's charging/discharging scenario is linked to its capacity and management, which unswervingly determines the expanse of regulatory work allocated to the EV [25]. The regulatory management is determined by the capacity and power-load mismatch. Moreover, EVs that engage in regulatory actions necessitate adequate time to charge the batteries to the expected level. As all generating units comprising EVs takes care of the regulation, any power imbalance will be divided into two portions. One component of the task will be done by all of the generating units in a certain location, with the remainder handled by BCM. Equations (2) and (3) are utilized to compute the maximum and minimum output power.

$$P_{AG}^{max} = + \left(\frac{1}{N_{EV}} \right) (\Delta P_{EVI}) \tag{2}$$

$$P_{AG}^{min} = - \left(\frac{1}{N_{EV}} \right) (\Delta P_{EVI}) \tag{3}$$

Where, N_{EV} is the EV quantity, ΔP_{EVI} is the incremental power variation in EVs, P_{AG}^{max} is the extreme output power and P_{AG}^{min} is least power output of EVs.

3 Bio-geography Based Krill Herd (BBKH) Optimization Technique

The authors in [50] gave the BBKH optimization concept. The krill herd (KH) approach is based on the krill swarm behaviour and is used to address

optimization problems. Three things in KH have the most influence on the situation.

- Other krill have an influence on their migration.
- Hunt exploit
- Physical diffusion

The lagrangian model is used in the following way inside a defined search space:

$$\frac{dY_i}{dt} = P_i + Q_i + R_i \tag{4}$$

Where, the movement generated by other krills is denoted by P_i, the hunt action is denoted by Q_i and the erratic diffusion is denoted by R_i. The first part's direction is defined by factors such as target impact, local impact, and repellant impact. The definition is presented as:

$$P_i = P^{max}\alpha_i + \omega_n P_i^{old} \tag{5}$$

Where, P^{max}, ω_n, P_i^{old} are maximum speed, inertia mass and last movement.

The second one, Q_i, is calculated using two variables: food position and previous experience, reported below:

$$Q_i = S_f\beta_i + \omega_f Q_i^{old} \tag{6}$$

Where,

$$\beta_i = \beta_i^{food} + \beta_i^{Best} \tag{7}$$

And S_f represents foraging speed, ω_f represents mass inertia and Q_i^{old} is final one.

The final one is an erratic process that is calculated using the highest diffusion speed and an erratic directional vector, which is expressed as:

$$R_i = R^{max}\gamma \tag{8}$$

where, R^{max} represents the largest diffusion speed and γ represents the random directional vector.

Hence, KH location from t to $t + \Delta t$ is estimated as:

$$Y_i(t+\Delta t) = Y_i t + \frac{dY_i}{dt} \tag{9}$$

The KH can carry out exploration quickly and locate the most favourable position. KH, on the other hand, has a limited capability for exploitation.

```
Begin
    Select krill i (its position Yi) with probability based on λi
    if rand (0,1) < λi then
  for j=1 to d (all elements) do
    Select Yj with probability based on μj
    if rand (0,1) < μj then
        Randomly select an element r from Yj
        Replace a random element in Yi with σ
    end if
  end for j
  end if
End.
```

Figure 4   Algorithm 1: Krill Migration (KM) operator [50].

The krill migration (KM) operator is combined with the krill herd technique to provide an effective BBKH optimization approach that overcomes the constraints of the krill herd technique. In BBKH, the KM operator is in charge of controlling the new krill herd solution for each krill. This improved search method might increase population variety and help krill design a small prospective zone more carefully at a later stage of the process, avoiding early convergence. The KM operator procedure are illustrated in algorithm 1, presented in Figure 4.

Due to its quick convergence, krill herd is utilised in BBKH to limit the krill cluster to a confined area. After that, a KM operator with the best exploitation is used to hunt locally for the best krill. The KH in BBKH concentrates on early optimization exploration, whereas the KM operator emphasizes on later optimization exploration, causing the majority of krill to gather around the ideal solution. As a result, BBKH uses the KH operator to fully explore the region while simultaneously taking use of the crucial information offered by the KM operator. Hence, the BBKH approach can overcome the KH's low exploitation. Figure 5 shows the steps used for tuning the controller gains for the present study using BBKH optimization technique.

4 Cascaded PI-MSPID Controller

Cascaded controller's concept originated from the sequential processes where the outcome of interior loop is supplied as an input to the outer loop. The measurement variables are related to both the loops of the system. The main
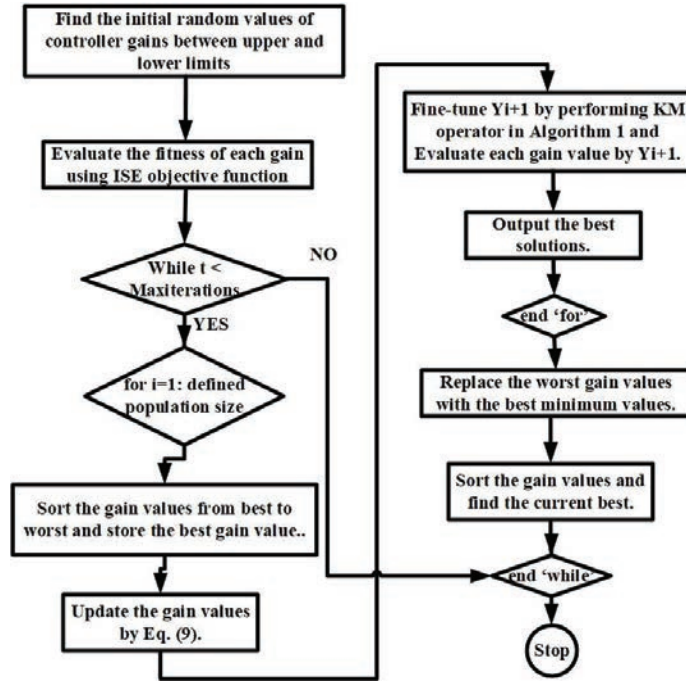
Figure 5 Algorithm 2: BBKH technique [50].

characteristics of cascaded controller as described in [35, 36] are mentioned below.

I. The effect of perturbations given to the outer process in succession is muted by inner measurement.
II. The measurement of the outer processes governs the ultimate output quality.

The prime objective of the cascaded controllers is to retort rapidly to disruptions before they scatter to other plant sections. The Figure 5 reports the structure of Cascaded PI-MSPID controller. The Equations (10) and (11) reports the transfer function equations of PI and MSPID controller.

$$F_1(s) = G_{Pi}(s) + \frac{G_{Ii}(s)}{s} \tag{10}$$

$$F_2(s) = \left(G_{Pi}(s) + \frac{sG_{Di}(s)}{\frac{1}{sN_{i\ (s)}+1}} \right) \left(G_{Pi}(s) + \frac{G_{Ii}(s)}{s} \right) \tag{11}$$
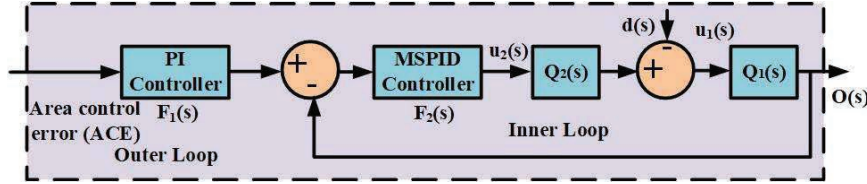
Figure 6 Cascaded PI-MSPID controller structure.

The loop (outer- $Q_1(s)$) of cascaded PI-MSPID controller contains the plant to be controlled. The prime focus of $Q_1(s)$ is to track the reference, area control error (ACE) against any load disturbance d(s). Hence, the present study incorporates PI controller in outer loop. The loop (inner – $Q_2(s)$) of the proposed secondary controller comprises of several generation sources. Its main aim is to lessen the system modelling impact and considerably improve the system performance. Henceforth, the MSPID controller is incorporated in its inner loop with high proportional and derivative gains to achieve reckless disruptions. The equation given in (12) reports the transfer function of cascaded PI-MSPID controller depicted in Figure 6.

$$O(s) = \left[\frac{Q_1(s)Q_2(s)\,F_1(s)\,F_2(s)}{1 + Q_1(s)Q_2(s)F_2(s)} \right] ACE(s) - \left[\frac{Q_1(s)}{1 + Q_1(s)Q_2(s)F_2(s)} \right] d(s) \tag{12}$$

5 Result and Discussion

MATLAB Simulink software is utilized to simulate the developed two-area DG based power system and execute the BBKH optimization algorithm. The concurrent system dynamic control is recognized in the present study. Area-1 is supplied with a step load perturbation (SLP) of 1%.

5.1 Optimal Controller Selection

In this section, optimal secondary controller is chosen from different controllers considered. Several controllers viz. PID, MSPID, cascaded PI-PID and cascaded PI-MSPID are inspected separately in DG and EV based power system. BBKH optimization approach is employed to optimize the controller gains. The developed system is simulated for each controller mentioned above. The responses for frequency and tie-line power in both areas are achieved and displayed in Figure 7. The Table 1 reports the optimized gains
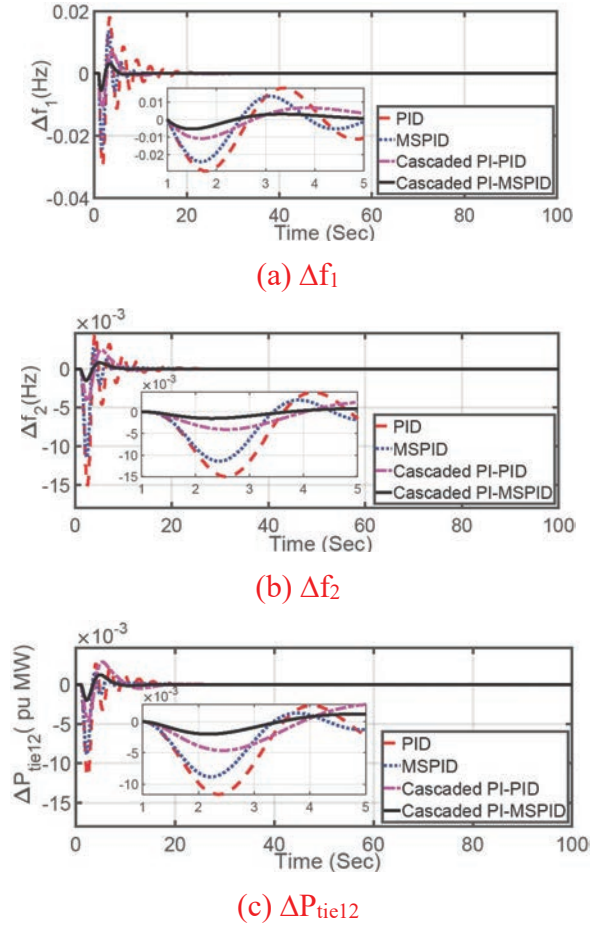
(a) Δf_1

(b) Δf_2

(c) ΔP_{tie12}

Figure 7   Comparison of several secondary controllers.

of different controllers. The comparison of responses in Figure 7 exposes better performance with cascaded PI-MSPID, as the responses achieved for cascaded PI-MSPID controller are non-oscillatory with lesser value of overshoot, undershoot and better response settling (Table 2). The supremacy of cascaded PI-MSPID controller is validated as it possesses very low deviations to disturbance and forces the output responses to zero when any disturbance is applied to the system. Further, the ISE values mentioned in Table 1 validates the supremacy of cascaded PI-MSPID controller. The Figure 8 reports the convergence curve achieved for different secondary controllers considered in terms of ISE values optimized with BBKH optimization approach.

Table 1 BBKH optimized secondary controller gains and their ISE values

Controller	G_{I11} G_{I12}	G_{I21} G_{I22}	G_{D11}	G_{D21}	N_{11}	N_{21}	G_{P11} G_{P12} G_{P13}	G_{P21} G_{P22} G_{P23}	ISE
PID	0.97	0.03	0.01	0.03	23.87	85.93	0.07	0.14	0.0012218
MSPID	1.32	0.69	0.11	0.19	84.59	10.13	0.98 0.95	0.61 0.53	0.0006521
Cascaded PI-PID	1.72 0.52	1.64 0.65	0.56	0.99	77.09	31.38	0.50	0.24	7.926e-05
Cascaded PI- MSPID	1.99 1.67	1.58 1.31	0.79	0.85	48.56	87.37	1.08 0.77 1.56	1.64 1.19 1.97	**3.40e-05**

Table 2 Observations of Figure 7

| Parameter	Controller	PU	PO	ST
Δf_1	PID	−0.0295	0.0180	25.4
	MSPID	−0.0242	0.0134	17.4
	Cascaded PI-PID	−0.0108	0.0067	15.2
	Cascaded PI-MSPID	**−0.0054**	**0.0031**	**8.57**
Δf_2	PID	−0.0150	0.0047	24.4
	MSPID	−0.0114	0.0028	22.5
	Cascaded PI-PID	−0.0041	0.0024	15.8
	Cascaded PI-MSPID	**−0.0015**	**0.0007**	**9.72**
$\Delta P_{tie\text{-}error}$	PID	−0.0116	0.0026	22.6
	MSPID	−0.0088	0.0014	19.4
	Cascaded PI-PID	−0.0046	0.0028	18.1
	Cascaded PI-MSPID	**−0.0019**	**0.0012**	**12.2**
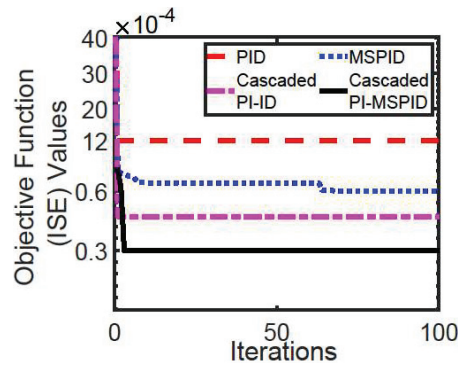
Figure 8 Convergence characteristics of different secondary controllers.

5.2 Flywheel Energy Storage (FES) Influence on System Dynamics

Renewable generation sources are majorly preferred at present times due to which energy storage becomes a major concern. Therefore, energy storage devices (ESD) have to play a major role in today's power system. ESDs have high capability to decrease frequency fluctuations and stabilize systems impacted by the system transients. In this respect, flywheel energy storage (FES) as ESD is placed in both areas. The power system in presence of FES is simulated utilizing optimal cascaded PI-MSPID controller. The system responses for FES based HPS are achieved and represented in Figure 9. The Table 3 reports the optimized gains of cascaded PI-MSPID controller. The investigation of Figure 9 discloses the intended performance of the HPS in the presence of FES. Further, the values noted for minimum value and

(a) Δf_1
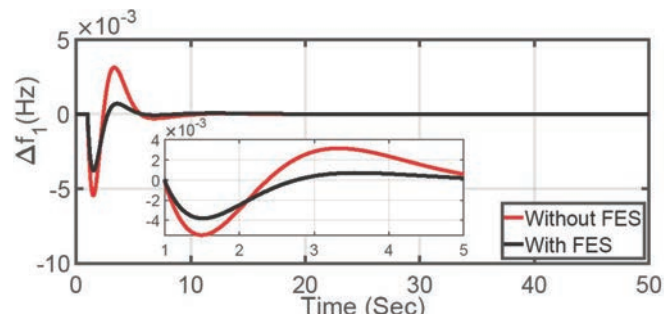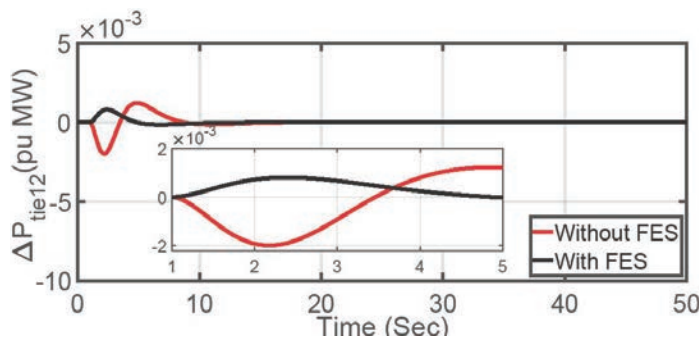
(b) ΔP_{tie12}

Figure 9   Response comparison in presence and absence of FES.

Table 3 BBKH optimized cascaded PI-MSPID controller gains

FES	PI Controller		MSPID Controller	
Proportional gain	G_{P11}	1.49	G_{P12}	1.23
			G_{P13}	1.43
	G_{P21}	0.36	G_{P22}	1.68
			G_{P23}	1.30
Integral gain	G_{I11}	0.01	G_{I12}	2.27
	G_{I21}	1.57	G_{I22}	1.96
Derivative gain		–	G_{D11}	1.22
			G_{D21}	1.75
Filter Coefficient		–	N_{11}	79.26
			N_{21}	72.44

Table 4 Observations of Figure 9

| Parameter	Combination	PU	PO	ST
Δf_1	Without FES	−0.0054	0.0031	8.57
	With FES	**−0.0038**	**0.0007**	**8.17**
Δf_2	Without FES	−0.0015	0.0007	9.72
	With FES	**−0.0010**	**0.0001**	**9.71**
$\Delta P_{tie\text{-}error}$	Without FES	−0.0019	0.0012	12.2
	With FES	**−0.0001**	**0.0008**	**10.4**

maximum value of the responses achieved in Table 4 validates the better performance in existence of FES.

5.3 EVs Effect on System Stability

EVs are being frequently used in present times due to fast depleting conventional sources. EVs have been able to improve the power system dynamics significantly [35] due to its rapid characteristics. To analyse the EVs influence in developed power system, EV in area-1 and area-2 are removed. The system dynamics under this condition are achieved and compared with the responses previously attained with EVs existing in the system as presented in Figure 10. The Table 5 reports the optimized gains of cascaded PI-MSPID controller without EVs. The understandings from Figure 10 reports the substantial performance in existence of EVs. Further, the values for undershoot, overshoot and settling time of the response in Table 6 validates the better performance with EVs in the system. This is because EVs serve as supportive energy storage devices and high frequency elements that emerge in established power system are properly addressed by EVs.

(a) Δf_1
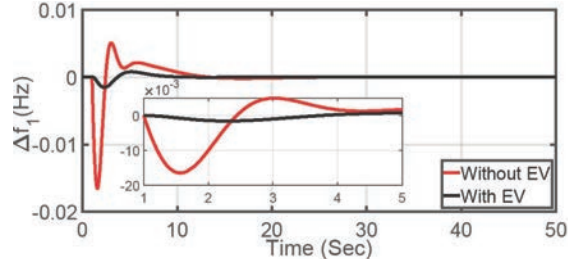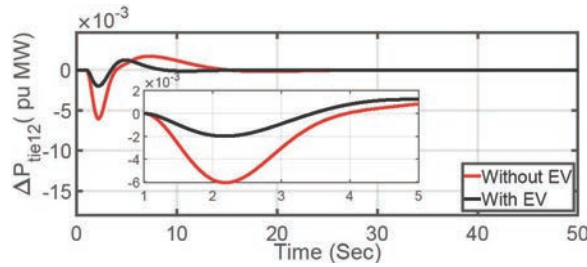
(b) ΔP_{tie12}

Figure 10   Response comparison in presence and absence of EV.

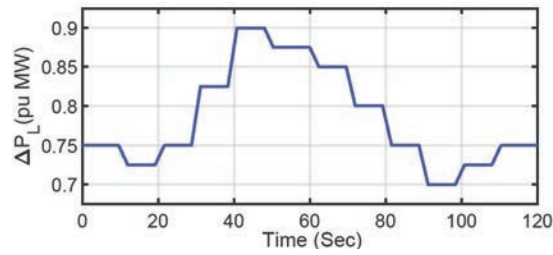**Table 5**   BBKH optimized cascaded PI-MSPID controller gains in absence of EVs

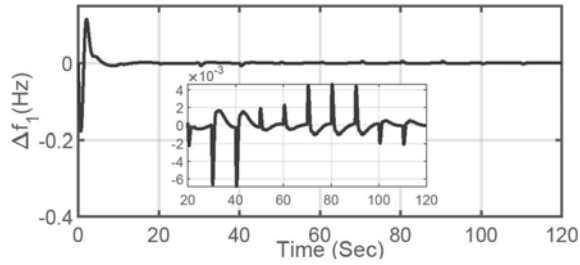| WTOTEVS	PI Controller		MSPID Controller	
Proportional gain	G_{P11}	0.93	G_{P12}	0.94
			G_{P13}	0.89
	G_{P21}	0.59	G_{P22}	0.01
			G_{P23}	0.68
Integral gain	G_{I11}	0.65	G_{I12}	0.57
	G_{I21}	0.98	G_{I22}	0.36
Derivative gain		–	G_{D11}	0.07
			G_{D21}	0.99
Filter Coefficient		–	N_{11}	31.44
			N_{21}	80.92

5.4 Practical Load Variations

In this study, the developed HPS is provided with a practical random load disturbance (ΔP_L) to check the system behaviour. The data is taken from reference number [51]. The practical load variations (ΔP_L) with respect to time (120s) is depicted in Figure 11(a). The developed DG and EV based
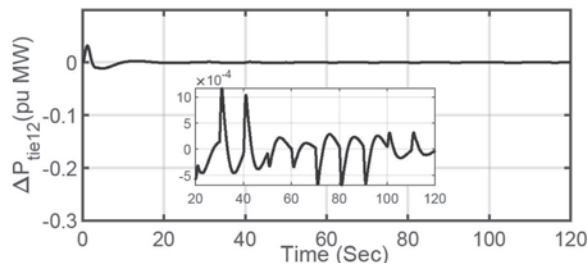
Table 6 Observations of Figure 10

Parameter	Controller	PU	PO	ST
Δf_1	Without EV	-0.0165	0.0050	14.3
	With EV	**-0.0054**	**0.0031**	**8.57**
Δf_2	Without EV	-0.0057	0.0017	16.8
	With EV	**-0.0015**	**0.0007**	**9.72**
$\Delta P_{tie\text{-}error}$	Without EV	-0.0061	0.0017	16.9
	With EV	**-0.0019**	**0.0012**	**12.2**

(a) Load Pattern


(b) Δf_1

(c) ΔP_{tie12}

Figure 11 Random load input and responses.

Table 7   BBKH optimized cascaded PI-MSPID controller gains in presence of random load deviations

RLP	PI Controller		MSPID Controller	
Proportional gain	G_{P11}	0.72	G_{P12}	1.12
			G_{P13}	0.85
	G_{P21}	1.48	G_{P22}	0.84
			G_{P23}	0.25
Integral gain	G_{I11}	0.83	G_{I12}	0.74
	G_{I21}	1.13	G_{I22}	1.05
Derivative gain		–	G_{D11}	0.05
			G_{D21}	0.58
Filter Coefficient		–	N_{11}	30.75
			N_{21}	65.36
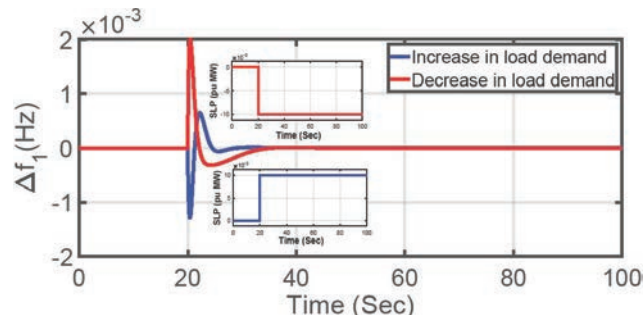
Figure 12   Effect of increase and decrease in load demand.

HPS in presence of optimal cascaded PI-PID controller is simulated for these erratic load alterations. The system responses for frequency & tie-line power are achieved, and displayed in Figure 11(b)–11(c), while as the Table 7 reports the optimized cascaded PI-MSPID controller gains. The detailed valuation of Figure 11(b)–11(c) exhibits robust performance of the developed system under defined ranges with rapid settling of responses following each variation in demand.

5.5 Effect of Increase and Decrease in Load Demand

In this analysis, the performance of optimal cascaded PI-MSPID controlled hybrid power system is tested by increasing and decreasing the load demand to the power system. Figure 12 shows the frequency response of area-1 with respect to the variation in load demand at time (t = 20s). The observations from Figure 12 shows that with the decrease in load demand, the frequency

starts to increase. The response is forced to steady state using the optimal controller very quickly and vice versa.

6 Conclusion

The present paper endorses the optimal performance of a cascaded PI-MSPID controller in a DG and EV based two-area power system. The concurrent dynamic control of frequency and tie-line power control is efficaciously recognized. The maximum and minimum value of the responses for cascaded PI-MSPID controller are significantly improved with respect to other controllers in addition to the improved settling of responses. The incorporation of flywheel energy storage and EVs in present work further enhances the performance of the power system. Further, the optimal cascaded PI-MSPID controller effectively takes care of practical load variations within defined limits of stability.

Appendix

Nominal system parameters:

f = 60 Hz; D_i = 8.33 ×10-3 p.u.MW/Hz; Hi = 5s; K_{pi} = 120 Hz/(p.u.MW); $Bias_i = \beta_i$ = 0.425 p.u.MW/Hz; T_{Pi} = 20s; R_i = 2.4 Hz/p.u.MW; loading = 50%;

Thermal unit: T_{ti} = 0.3s, T_{gi} = 0.08s, T_{ri} = 10s, K_{ri} = 0.5.

Geo-Thermal Unit: g = 0.05, t = 0.1.

Electric vehicle: N_{EVi} = 1, K_{EVi} = 1, T_{EVi} = 1s.

Flywheel energy storage: K_{FES} = −0.01; T_{FES} = 0.1s.

Solar thermal system unit : K_{STS} = 1; T_{STS} = 1.

Wind turbine system: K_{WTS} = 1; T_{WTS} = 1.5.

References

[1] Z. Farooq, A. Rahman, S.A. Lone, 'Load frequency control of multi-source electrical power system integrated with solar-thermal and electric vehicle,'Int Trans Electr Energ Syst., 31: e12918. https://doi.org/10.1002/2050-7038.12918, 2021.

[2] O.I. Elgerd, C.E. Fosha, 'Optimum megawatt-frequency control of mul-tiarea electric energy systems', IEEE Transactions on Power Apparatus System PAS-89(4), pp. 556–563, 1970.

[3] Z. Farooq, A. Rahman and S. A. Lone, 'Fuzzy and MBO optimized Load Frequency Control of hybrid Power System,' 2021 IEEE 18th India Council International Conference (INDICON), 2021, pp. 1–6, doi: 10.1 109/INDICON52576.2021.9691624.

[4] S. Safiullah, A. Rahman, M. A. Aftab and S. M. Suhail Hussain, 'Per-formance study of ADRC and PID for concurrent Frequency-Voltage Control of Electric Vehicle Incorporated Hybrid Power System,' 2022 IEEE International Conference on Power Electronics, Smart Grid, and Renewable Energy (PESGRE), 2022, pp. 1–6, doi: 10.1109/PESGRE52 268.2022.9715937.

[5] R. K. Sahu, S. Panda, U. K. Rout, 'Teaching learning based opti-mization algorithm for automatic generation control of power system using 2-DOF PID controller', International Journal of Electric Power & Energy Systems, 31, pp. 287–301, 2016.

[6] L. C. Saikia, J. Nanda, S. Mishra, 'Performance comparison of several classical controllers in AGC for multi-area interconnected thermal sys-tem', International Journal of Electrical Power & Energy Systems, 33, pp. 394–401, 2011.

[7] J. Nanda, S. Mishra, L. C. Saikia, 'Maiden application of bacterial for-aging based optimization technique in multi area automatic generation control', IEEE Transanctions on Power Systems, 24, pp. 602–609, 2009.

[8] Y. Wang, R. Zhou,C. Wen, 'New robust adaptive load-frequency control with system parametric uncertainties', IEE Proceedings – Generation, Transmission and Distribution., 141, (3), pp. 184–190, 1994.

[9] K. R. Sudha, R.V. Shanthi, 'Load frequency control of an interconnected reheat thermal system using type-2 fuzzy system including SMES units', International Journal of Electrical Power & Energy Systems, 43(1), pp. 1383–1392, 2012.

[10] P. Dash, L. C. Saikia, N. Sinha, 'Flower pollination algorithm optimized PIPD cascade controller in automatic generation control of a multi-area power system', International Journal of Electrical Power & Energy Systems, 82, pp. 19–28, 2016.

[11] J. Nanda, A. Mangla, S. Suri, 'Some new findings on automatic gener-ation control of an interconnected hydrothermal system with conven-tional controllers', IEEE Transactions on Energy Conversion, 21(1), pp. 187–194, 2006.

[12] M. L. Kothari, J. Nanda, 'Application of optimal control strategy to automatic generation control of a hydrothermal system', IEE Proceedings D (Control Theory and Applications), 135(4), pp. 268–274, 1988.

[13] D. Saha, L. C. Saikia, 'Performance of FACTS and energy storage devices in a multi area wind-hydro-thermal system employed with SFS optimized I-PDF controller', Journal of Renewable and Sustainable Energy, 9(2), pp. 1–19, 2017.

[14] I. Hussain, S. Ranjan, D. C. Das, et al, 'Performance analysis of flower pollination algorithm optimized PID controller for wind-PV-SMES-BESS diesel autonomous hybrid power system', International Journal of Renewable Energy Research-IJRER 7(2), pp. 643–651, 2017.

[15] M. Raju, L. C. Saikia, N. Sinha, 'Load frequency control of multi-area hybrid power system using symbiotic organisms search optimized two degree of freedom controller', International Journal of Renewable Energy Research-IJRER, 7(4), pp. 1663–1674, 2017.

[16] S. K. Pandey, S. R. Mohanty, N. Kishor, et al., 'Frequency regulation in hybrid power systems using particle swarm optimization and linear matrix inequalities based robust controller design', International Journal of Electrical Power & Energy Systems, 63, pp. 887–900, 2014.

[17] D. Das, A. Roy and N. Sinha, 'GA based frequency controller for solar thermal–diesel–wind hybrid energy generation/energy storage system', International Journal of Electrical Power & Energy Systems, 43(1), pp. 262–279, 2012.

[18] W. Tasnin, L. C. Saikia, Comparative performance of different energy storage devices in AGC of multi-source system including geothermal power plant', Journal of Renewable and Sustainable Energy, 10, pp. 024101, 2018.

[19] C. F. Lu, C. C. Liu, C.J. Wu, 'Effect of battery energy storage system on load frequency control considering governor dead band and generation rate constraint', IEEE Transactions on Energy Conversion, 10(3), pp. 555–561, 1995.

[20] M. Ponnusamy, B. Banakara, S. S. Dash, et al., 'Design of integral controller for load frequency control of static synchronous series compensator and capacitive energy source based multi area system consisting of diverse sources of generation employing imperialistic competition algorithm', International Journal of Electrical Power & Energy Systems, 73, pp. 863–871, 2015.

[21] A. Pappachen, A. P. Fathima, 'Load frequency control in deregulated power system integrated with SMES–TCPS combination using ANFIS

controller', International Journal of Electrical Power & Energy Systems, 82, pp. 519–534, 2016.

[22] M. Cheng, S. Sami and J. Wu, 'Benefits of using virtual energy storage system for power system frequency response', Applied Energy, 194, pp. 376–385, 2017.

[23] H. Liu, K. Huang, Y. Yang, H. Wei and S. Ma, 'Real-time vehicle-to-grid control for frequency regulation with high frequency regulating signal', Protection and Control of Modern Power Systems, 3(1), pp. 1–8, 2018.

[24] S. Safiullah, A. Rahman, S.A. Lone, 'State-observer based IDD controller for concurrent frequency-voltage control of a hybrid power system with electric vehicle uncertainties,' Int Trans Electr Energ Syst., 31(11): e13083. doi:10.1002/2050-7038.13083, 2021.

[25] S. Safiullah, A. Rahman, S.A. Lone, 'Optimal control of electrical vehicle incorporated hybrid power system with second order fractional-active disturbance rejection controller,' Optim Control Appl Meth., 1–30. doi:10.1002/oca.2826, 2021.

[26] K.P. Singh Parmar, S. Majhi, D.P. Kothari, 'Load frequency control of a realistic power system with multi-source power generation', International Journal of Electrical Power & Energy Systems, 42(1), pp. 426–433, 2012.

[27] M. Kazemi, M. Karrari and M. Menhaj, 'Decentralized robust adaptive-output feedback controller for power system load frequency control', Electrical Engineering, 84(2), pp. 75–83, 2002.

[28] M. Azzam, 'Robust automatic generation control', Energy Conversion and Management, 40(13), pp. 1413–1421, 1999.

[29] M. Ebrahim, M. Becherif and A. Abdelaziz, 'PID-/FOPID -based frequency control of zero-carbon multisources-based interconnected power systems under deregulated scenarios', International Transactions on Electrical Energy Systems, 31(2), 2020.

[30] B. Sonker, D. Kumar and P. Samuel, 'Design of two degree of freedom-internal model control configuration for load frequency control using model approximation', International Journal of Modelling and Simulation, 39(1), pp. 27–37, 2018.

[31] J. Singh, K. Chattterjee and C. Vishwakarma, 'Two degree of freedom internal model control-PID design for LFC of power systems via logarithmic approximations', ISA Transactions, 72, pp. 185–196, 2018.

[32] D. Sharma and S. Mishra, "Disturbance-Observer-Based Frequency Regulation Scheme for Low-Inertia Microgrid Systems", IEEE Systems Journal, 14(1), pp. 782–792, 2020.

[33] A. Dev, S. Anand and M. Sarkar, 'Nonlinear disturbance observer based adaptive super twisting sliding mode load frequency control for non-linear interconnected power network', Asian Journal of Control, 23(5), pp. 2484–2494, 2020.

[34] A. Kumar, M. Anwar and S. Kumar, 'Sliding mode controller design for frequency regulation in an interconnected power system', Protection and Control of Modern Power Systems, 6(1), 2021.

[35] Z. Farooq, A. Rahman and S. A. Lone, 'System dynamics and control of EV incorporated deregulated power system using MBO-optimized cascaded ID-PD controller', International Transactions on Electrical Energy Systems, 31(11), 2021.

[36] Z. Farooq, A. Rahman, S.M.S. Hussain, T.S. Ustun, 'Power Generation Control of Renewable Energy Based Hybrid Deregulated Power System,' Energies, *15*, 517. https://doi.org/10.3390/en15020517, 2022.

[37] Z. Farooq, A. Rahman and S. A. Lone, 'Power generation control of restructured hybrid power system with FACTS and energy storage devices using optimal cascaded fractional-order controller,' Optim Control Appl Meth., 1–30. doi:10.1002/oca.2850, 2022.

[38] M. Mohamed, A. Diab, H. Rezk and T. Jin, 'A novel adaptive model predictive controller for load frequency control of power systems integrated with DFIG wind turbines', Neural Computing and Applications, 32(11), pp. 7171–7181, 2019.

[39] D. Rangaswami and P. Sennappan, 'Load frequency control using multi-stage fuzzy logic controller for wind-micro hydro-diesel hybrid power system', Journal of Vibration and Control, 19(7), pp. 1004–1014, 2012.

[40] Nikhil Pathak, Ashu Verma, Terlochan Singh Bhatti, Ibraheem Nasiruddin, Haocheng Luo & Zechun Hu, 'Generation Rate Constraints Physical Identification and Modeling in AGC of Multi-Area Power Systems', Electric Power Components and Systems, 47:11-12, pp. 966–984, 2019.

[41] S. Abd-Elazim and E. Ali, 'Load frequency controller design of a two-area system composing of PV grid and thermal generator via firefly algorithm', Neural Computing and Applications, 30(2), pp. 607–616, 2016.

[42] B. Dhanasekaran, S. Siddhan and J. Kaliannan, 'Ant colony optimization technique tuned controller for frequency regulation of single area nuclear power generating system', Microprocessors and Microsystems, 73, p. 102953, 2020.

[43] M. Sobhy, A. Abdelaziz, H. Hasanien and M. Ezzat, 'Marine predators algorithm for load frequency control of modern interconnected power

systems including renewable energy sources and energy storage units', Ain Shams Engineering Journal, 12(4), pp. 3843–3857, 2021.

[44] H. Hasanien and A. El-Fergany, 'Symbiotic organisms search algorithm for automatic generation control of interconnected power systems including wind farms', IET Generation, Transmission & Distribution, 11(7), pp. 1692–1700, 2016.

[45] D. Guha, P. Roy and S. Banerjee, 'Symbiotic organism search algorithm applied to load frequency control of multi-area power system', Energy Systems, 9(2), pp. 439–468, 2017.

[46] D. Guha, P. Roy and S. Banerjee, 'Application of backtracking search algorithm in load frequency control of multi-area interconnected power system', Ain Shams Engineering Journal, 9(2), pp. 257–276, 2018.

[47] S. Singh, T. Prakash, V. Singh and M. Babu, 'Analytic hierarchy process based automatic generation control of multi-area interconnected power system using Jaya algorithm', Engineering Applications of Artificial Intelligence, 60 (2), pp. 35–44, 2017.

[48] D. Guha, P. Roy and S. Banerjee, 'Load frequency control of interconnected power system using grey wolf optimization', Swarm and Evolutionary Computation, 27, pp. 97–115, 2016.

[49] R. Bhatt, G. Parmar, R. Gupta, 'Whale optimized PID controllers for LFC of two area interconnected thermal power plants', ICTACT Journal on Microelectronics (IJME). 3(4) 467–472, 2018.

[50] G.-G. Wang, A. H. Gandomi and A. H. Alavi, 'an effective krill herd algorithm with migration operator in biogeography-based optimization', Applied Mathematical Modelling, 38(9), pp. 2454–2462, 2014.

[51] AK Barik, DC Das, 'Coordinated regulation of voltage and load frequency in demand response supported biorenewable cogeneration-based isolated hybrid microgrid with quasi-oppositional selfish herd optimisation' Int Trans Electr Energy Syst. 30(1):e12176. 2020.

[52] F. Fayaz & G. L. Pahuja, 'Disturbance Rejection Based Controller for Frequency Control of Restructured Power System,' IETE Journal of Research, DOI: 10.1080/03772063.2021.2021824, 2022

Biographies

Farhana Fayaz graduated in 2014 from BGSB University, Rajouri, J& K, India and obtained Master of Engineering and Technology in Power System Engineering. At present, she is pursuing PhD from NIT Kurukshetra, Haryana, India in EED. Her research interests include Load Frequency Control, Power System Protection and Power System Reliability.

Gobind Lal Pahuja has done his M.Tech and Ph. D from NIT Kurukshetra (Previously REC) Haryana, India. At presesnt, he serving as an professor in EED, NIT Kurukshetra. The research interests are optimization of control system, power system reliability, soft computing. He has published many research papers in reputed journals.